TPX2 Induces Mitotic Survival via *BCL2L1* Induction Through YAP1 Protein Stabilization in Human Embryonic Stem Cells

Yun-Jeong Kim
Seoul National University
Young-Hyun Go
Sogang University
Ho-Chang Jeong
Sogang University
Seong-Min Kim
Seoul National University
Hyun Sub Cheong
Sookmyung Women's University
Hyoung Doo Shin
Sogang University
Haeseung Lee
Korea Institute of Oriental Medicine
Hyuk-Jin Cha (hjcha93@snu.ac.kr)
Seoul National University https://orcid.org/0000-0001-9277-2662

Research Article

Keywords: TPX2, AURKA, YAP1, BCL2L1, mitotic stress, culture adaptation, human embryonic stem cells, mitotic survival

Posted Date: June 28th, 2021

DOI: https://doi.org/10.21203/rs.3.rs-626430/v1

Abstract

Genetic alterations have been reported in most human embryonic stem cells (hESCs) for decades. 'Survival advantage,' a typical trait acquired during long-term *in vitro* culture, results from induction of *BCL2L1* upon frequent copy number variation (CNV) at locus 20q11.21 and is one of the strongest candidates associated with genetic alteration via escape from mitotic stress. However, the underlying mechanisms for *BCL2L1* induction remain undefined. Furthermore, abnormal mitosis and 'survival advantage' frequently occurring in the late passage are respectively associated with the expression of TPX2 and *BCL2L1*, which are located in locus 20q11.21. In this study, we observed that 20q11.21 CNV was not sufficient for *BCL2L1* induction and consequent survival traits in pairs of hESCs and human induced pluripotent stem cells (iPSCs) with normal and 20q11.21 CNVs. Inducible expression of TPX2 and basal TPX2 expression due to leakage of the inducible system in hESCs with normal copy number was sufficient to promote *BCL2L1* expression and promoted high tolerance to mitotic stress. High Aurora A kinase activity by TPX2 stabilized YAP1 protein to promote YAP1 dependent *BCL2L1* expression. Thus, a chemical inhibitor of Aurora A kinase and knockdown of YAP/TAZ significantly abrogated the aforementioned high tolerance to mitotic stress through *BCL2L1* suppression. These results suggest that the collective expression of *TPX2* and *BCL2L1* from CNV at loci 20q11.21 and a consequent increase in YAP1 signaling would promote genome instability during long-term *in vitro* hESC culture.

Introduction

Due to their pluripotency, human embryonic stem cells (hESCs) have great potential in stem cell-based cell therapy; however, their frequent genetic aberrations during *in vitro* maintenance are considered a major hurdle that compromises the safety of stem cell-based therapy[1, 2]. However, despite these concerns [3], few studies have explored the biological consequences, risks, and biomarkers of hESC genetic alterations[4]. As demonstrated by several massive genomic studies, copy number variations (CNVs) occur most frequently during the sub-chromosomal amplification of locus 20q11.21 and trisomy of chromosome 12 or 17 [5] [6, 7].

One of the most characteristic phenotypic changes of genetically aberrant hESCs is 'culture adaptation' [5], which is an acquired survival trait (also referred to as 'survival advantage') under various stress conditions such as culture, genotoxic stress, and single-cell dissociation, among others[8, 9]. Such acquired survival trait results from induction of *BCL2L1* due to amplification of 20q11.21 [10] (encoding BCL-xL), a typical anti-apoptotic gene located at 20q11.21[8, 11] and/or dominant mutation in p53 [12], as the mitochondria are primed to cell death upon genotoxic stress through p53 translocation in hESCs [13–16]. A recent study revealed that escape from mitotic cell death during mitotic errors due to this acquired survival trait (either induction of *BCL2L1*, or dominant mutation of *NOXA*, a pro-apoptotic factor) leads to aneuploidy[9]. In this context, a targeting protein for Xklp2 (TPX2) also located in 20q11.21 was suggested to be the putative driver for abnormal mitosis by disrupting spindle dynamics[17]. However, despite the significance of 'survival advantage' in the phenotypic changes of culture-adapted hESCs and even aneuploidy, the molecular mechanisms underlying this phenomenon are not fully understood except

for *BCL2L1* induction. Moreover, a reduction in serum response factor (SRF) expression [18] or high oxygen concentrations during *in vitro* culture [19] have been associated with hESC genetic alterations.

To ensure genome integrity, hESCs become highly sensitive to genotoxic stress via mitochondrial priming to apoptosis [16]. However, the contemporaneous expression of anti-apoptotic factors maintains a fine balance between survival and apoptosis [20]. It is also worth noting that the deletion of Yap1 leads to embryonic lethality [21], thus suggesting that Yap1 is required for self-renewal and differentiation of mESCs [22]. A recent study demonstrated that Yap1 in mouse embryonic cell lines (ESCs) serves as a safeguard to attenuate mitochondrial apoptosis by upregulating typical anti-apoptotic factors including *BCL2L1*[23]. Similarly, Rho-dependent activation of YAP1 promotes long-term survival of hESCs [24]. In addition to ESCs, YAP1 activation in cancer cells elevates survival through the induction of *BIRC5* and *BCL2L1*, both of which are important for hESC survival[25].

In this study, using isogenic hESC with different passage numbers and CNV status, we demonstrated that a 20q11.21 CNV was insufficient not only for *BCL2L1* induction but also to induce 'acquired survival.' TPX2, located at locus 20q11.21, was highly induced in culture-adapted hESCs and conferred resistance under mitotic stress through *BCL2L1* induction. Our findings also revealed that YAP1 protein stabilization by Aurora A kinase activated by TPX2 induction was responsible for *BCL2L1* induction, which resulted in mitotic stress escape, suggesting that additional signaling (e.g., YAP1) would be required for determining culture adapted phenotypic changes in hESCs other than CNVs.

Materials And Methods

Reagents

The primary antibodies against α-tubulin (#sc- 8035), b-actin (#sc-47778), PARP (#sc-7150), YAP1/TAZ (#sc-101199), Vinculin(sc-25336), eGFP(sc-9996) were purchased from Santa Cruz Biotechnology, Inc. Antibodies against phospho-YAP1 (#4911s), Phospho-Aurora A (#3079), TPX2 (#12245) were purchased from Cell Signaling Technology. Bcl-xL (ab32370) is from Abcam, and Y-27632 (Peprotech#1293823) was purchased from Biogems. siRNAs targeting Negative Control (#SN-1003) and the others (listed in Table 2) were obtained from Bioneer. Expression vectors of 8X GTIIC-luciferase were kindly gifted by Prof. Mo Jung-Soon at Ajou University.

Cell culture

Human induced pluripotent stem cell line, hmiPS1 and hmiPS2 were provide by Korea National Stem Cell Bank (Korea National Health Institute). Human embryonic stem cell (WA09: H9, WiCell Research Institute, CHA3-hESCs) were maintained in iPSC-brew (Miltenyi biotechnology, #130-104-368) with 0.1% gentamycin (Gibco, Waltham, MA, USA, #15750-060) on a matrigel (Corning, Corning, NY, USA, #354277)-coated cell culture dish at 37℃ and humidified to 5% in a CO2 incubator. Cells were maintained with daily changed media and passaged every 5-6 days. Upon transfer, hESCs were rinsed with DPBS and detached enzymatically with Dispase (Life Technologies) followed by 3 times washed with DMEM/F-12

(Gibco #11320-033) media before plating. If needed 10 μM of Y27632 (Peprotech#1293823) was used for cellular attachment.

Transfection (Plasmid DNA and siRNA)

Cells were prepared about 1 x 106 per 100uL in Opti-MEM. Each cell was separated into cuvettes (EC-002) with plasmid DNA 2μg (or siRNA 100pmole) added per 100uL. Electroporation was done by NEPA21 super Electroporator. After electroporation, cells were seeded to Matrigel coated culture plate with 1 μM of Y27632, and cultured for 24hr~72hr before harvest. After 24 hours, the media was changed to fresh media without Y27632.

RNA extraction and Quantitative real-time PCR

Total RNA was extracted using easy-BLUE^{TM} Total RNA Extraction Kit (#17061, iNtRON), and dissolved in RNase-free DEPC-treated water. cDNA was made using extracted RNA and RT master mix (#RR036, TAKARA). Synthesized cDNA, TB green (#RR420, TAKARA), and primers were used as a template for examining the real-time PCR. (Primer list was shown in Table 1.) TAKARA's 2 step protocol was used by Light Cycler 480 Instrument II from Roche.

Immunoblotting

Cell lysates were extracted with RIPA buffer supplemented with a 1% protease inhibitor cocktail and 0.1% sodium orthovanadate. After 1-hour incubation on ice, total protein was extracted by centrifuge. The concentration of total protein was quantified by the BCA protein assay kit (#23225, Thermo ScientificTM). Approximately 25μg of total protein were separated on various (7.5%, 10%, 15%) concentrations of SDS-PAGE. Separated protein in the gel was transferred to the PVDF membrane. Membrane with protein was blocked with 5% skim milk in TBS-T (Tris-buffered saline with 0.1% Tween-20) for 1 hour and then washed by TBS-T for every 5 minutes three times. The membrane was incubated with the primary antibody in TBS-T (1:1000) with 0.1% sodium azide overnight, 4°C. The incubated membrane was washed for 5 minutes three times with TBS-T. The membrane was incubated with HRP-conjugated secondary antibody (Jackson Immunoresearch Laboratories) in TBS-T (1:10000) for 1 hour, room temperature. The incubated membrane was washed for 15 minutes three times with TBS-T. Immunoreactivity was detected by Chemi-Doc using WEST-QueenTM (#16026, iNtRON Biotechnology) kit. The band intensity was measured using Fusion FX software and normalized with the loading control.

Determining regions of copy number variation (CNV)

H9-iTPX2-mock, H9-iTPX2-Dox, and H9-P4 were genotyped using Illumina Asian Screening Array SNP-chip. Probe intensity values (Log R ratios) and B-allele frequency values were plotted using Illumina's GenomeStudio version 2.0.

Dual-luciferase assay

Cells were transfected with a specific promoter-luciferase vector and pRL vector using the above description. Cell lysates were extracted with 1X passive lysis buffer. After 1-hour incubation on ice, the total lysate was extracted by centrifuge. The supernatant was used for reaction with LARII and Stop & Glo reagent. The reporter assay was performed according to the Dual-Luciferase Reporter Assay System (#E1980, Promega).

Cell Death Assay

Cell death was analyzed by flow-cytometry. Regarding Annexin V/7-AAD staining, cells at 24 h after treatment of each flavonoid were washed twice with PBS and stained with FITC conjugated Annexin V antibody (BD Bioscience, Franklin Lakes, NJ, USA, #556419) and 7-AAD (BD Bioscience, #559925) or Propidium iodide(PI) for an additional 45–60 min at room temperature in the dark. Cells stained with Annexin V/7-AAD were analyzed by FACS Calibur (BD Bioscience). Concerning all of the bright field images captured, a Light channel optical microscope (Olympus, Tokyo, Japan, CKX-41) or JULI-stage (NanoEntek, Seoul, Korea) was used in accordance with the manufacturer's protocol.

Statistical analysis

Graphical data were presented as mean ±S.E.M. Statistical significance for more than three groups was determined using one-way or two-way analysis of variance (ANOVA) following a Tukey multiple comparison post-test. Statistical significance between the two groups was analyzed using unpaired Student’s t-tests. Statistical analysis was performed with GraphPad Prism 8 software (https://www.graphpad.com/scientific-software/prism/). Significance was assumed for $p<0.05$(*), $p<0.01$(**), $p<0.001$(***).

Results

The survival advantage of culture-adapted hESCs under mitotic stress

Culture-adapted hESCs become highly resistant to various stressors such as DNA damage[11], single-cell dissociation, and YM155[8], a stemtoxic agent that selectively induces death in undifferentiated pluripotent stem cells[13] through *SLC35F2*[26,27]. In addition to the increased survival of hESCs under genotoxic stress, escape from cell death during mitosis has been suggested to increase aneuploidy during long-term culture[9]. Thus, we examined whether P4 hESCs exhibiting the survival trait under YM155 treatment (Fig. 1A) due to BCL-xL induction (encoded by *BCL2L1,* Fig. 1B) were more resistant to mitotic stress compared to P1 hESCs. P1 or P4 hESCs were treated with typical mitotic drugs targeting mitotic spindles such as nocodazole (Noc), spindle destabilizer, and taxol (Tax), as well as a spindle stabilizer, after which cell death was evaluated. Similar to YM155, P4 hESCs were highly resistant to mitotic stress inducers (Figs. 1C and D).

20q11.21 CNV was not sufficient to induce the survival trait in hESCs

Except for the role of *BCL2L1* induction followed by CNV at locus 20q11.21 [10] or p53 dominant mutations [12], little is known regarding the mechanisms by which the survival trait is acquired during hESC culture adaptation. Further, no previous studies have determined how *BCL2L1* transcription becomes upregulated, thus resulting in the survival advantage trait in culture-adapted hESCs. We observed that the survival trait became manifested in P3 (over 200 passages) and P4 (over 300 passages), but not P2 (over 100 passages) (Fig. S1A) with *BCL2L1* expression comparable to that of P1 (up to 40 passage) hESCs [8], although CNV at locus 20q11.21 occurred in P2, P3, and P4 hESCs [8]. Similarly, hFmiPS1 (passage 20, normal iPSCs: hFmiPSC1-D1) and mutant cells (passage 30 with 20q11.21 CNV: hFmiPS2-DCB1) [28] underwent similar cell death by YM155 treatment (Fig. S1B) with comparable *BCL2L1* expression [28]. These results imply that the acquisition of the survival trait via *BCL2L1* induction may require additional events other than 20q11.21 CNV.

BCL2L1 induced survival associated with TPX2

As previously demonstrated, amplification of 20q11.21 was the most frequently occurring genome aberration and CNV of *ID1, BCL21L,* and *HM13* at locus 2011q.21, suggesting that this was a marker of genome aberration [5]. However, intriguingly, not all genes at locus 20q11.21 were transcriptionally active in hESCs having 20q11.21 CNV (e.g., P2, P3, and P4 hESCs) (Fig. 2A). Among the genes in the 20q11.21 locus, TPX2, which was previously shown to induce aberrant mitosis in culture-adapted hESCs[17], was concurrently induced with *BCL2L1* expression. Similarly, BCL-xL protein level was closely associated with TPX2 protein level in P3 and P4 hESCs where the survival trait was evident (Fig. 2C). Concretely, P4 hESCs with high TPX2 expression also expressed higher levels of *BIRC5* (encoding Survivin), an anti-apoptotic factor highly expressed in undifferentiated hESCs [13,29] along with *BCL2L1* (Fig. 2D). Considering the roles of TPX2 in cancer malignancy [30] and survival/chemoresistance [31], it is readily presumed that TPX2 expression may be associated with *BCL2L1* induction and consequent survival traits. As predicted, depletion of TPX2 in P4 hESCs significantly attenuated *BCL2L1* expression (Fig. 2E), suggesting that TPX2 induction somehow regulates *BCL2L1* expression and confers the survival trait. The doxycycline (Dox) inducible TPX2 cell line established from P1 hESCs (iTPX2-hESCs) was used to explore this possibility (Fig. S2A). TPX2 mRNA (Fig. S2A) and protein (Fig. S2B) induction occurred in a dose-dependent manner. The signal from green fluorescence protein (GFP) conjugated with TPX2 was evident in the mitotic spindle where TPX2 is located during mitosis [32] (Fig. S2C). Using the iTPX2-hESCs, we examined whether *BCL2L1* transcription was promoted by TPX2 induction with Dox. Surprisingly, TPX2 induction was sufficient to increase *BCL2L1* mRNA (Fig. 2F) in a dose-dependent manner (Fig. 2G), as well as protein (Fig. 2H). It is important to note that iTPX2-hESCs were established from P1 hESCs with normal copy numbers and therefore the copy number of iTPX2-hESCs remained normal regardless of Dox treatment unlike P4 hESCs (Fig. 2I).

TPX2 induction rescues mitotic cell death of normal hESCs

We have previously demonstrated that TPX2, located at locus 20q11.21 along with *BCL2L1*, would be a putative driver for abnormal mitosis[17]. Using iTPX2-hESCs, cell death under mitotic stress (e.g.,

Noc) was determined after TPX2 induction by doxycycline (Dox). We noted that only a portion of cells expressed GFP-TPX2 even after Dox treatment for unknown reasons. Thus, a GFP negative population was used as an internal control and the cell death of the GFP positive population (expressing TPX2) of iTPX2-hESCs was monitored after mitotic stress (Fig. 3A). As predicted, GFP positive cells (expressing TPX2) were more resistant to mitotic stress induced by Noc (Fig. 3A) and Tax (Fig. S3A) than GFP negative cells. Similar results were obtained in a dose-dependent manner (Fig. 3B). The resistance to the mitotic stress by TPX2 induction was reproduced in other iTPX2-hESCs derived from hCHA3 (Fig. S3B). To rule out the potential pro-survival effect of GFP expression (rather than TPX2), P1 expressing enhanced green fluorescent protein (EGFP-P1) was co-cultured with P4 or iTPX2 hESCs (Fig. 3C), as basal TPX2 level in P4 and iTPX2 (due to leakage of Tet-O system [33]) was comparably higher than that of P1 hESCs (Fig. S3C). Consistently, the hESCs with high TPX2 expression (e.g., P4 and iTPX2) were more resistant to Noc-induced mitotic stress regardless of GFP expression (Figs. 3D and E). Higher TPX2 in P4 hESCs than P1 hESCs occurred constantly regardless of cell cycle phase[17]. To further assess whether high TPX2 expression was responsible for the resistance to mitotic stress, TPX2 was transiently depleted by siRNA#3 (Fig. S3D). Depletion of TPX2 in P4 hESCs at a similar level of TPX2 in P1 hESCs (Fig. S3D), sensitized the cells to Noc induced mitotic stress (Fig. 3F). It is also worth noting that stable knockdown or expression of TPX2 in hESCs was unsuccessful even after multiple attempts, suggesting that the basal level of TPX2 is critical for self-renewal of hESCs.

YAP/TEAD4 leads to *BCL2L1* expression

Despite the occurrence of high mitochondrial priming to apoptosis[16], anti-apoptotic factors that are highly expressed in human undifferentiated ESCs such as *BIRC5*[13,29] maintain a fine balance between hESC life and death[20]. Particularly, *BIRC5* or *BCL2L1*, anti-apoptotic factors highly expressed in P4 hESCs (Fig. 2D) that are downstream of YAP1[25], were upregulated in P4 hESCs. Considering the key roles of YAP1 in the survival of ESCs[23,24], we hypothesized that YAP1 activity may account for the acquisition of survival traits in culture-adapted hESCs. It has been previously demonstrated that Rho and Hippo regulation on YAP/TAZ activation is critical for the survival response of hESCs [24]. Similarly, geneset for Hippo signaling was lesser enriched in P3 and P4 hESCs (showing culture adapted phenotypes) based on geneset enrichment analysis (GSEA) than P1 and P2 hESCs (showing high mitochondrial cell death) (Figs. 4A and S4A). YAP1 activity determined by GTIIC reporters was significantly higher in P4 hESCs (Fig. 4B). Considering the pivotal role of YAP1 in the survival of both mouse and human ESCs [23,24], high YAP1 activity acquired during *in vitro* culture could further enhance the survival signal, thus resulting in the survival advantage. Although YAP1 mRNA level itself remained unaltered, *BCL2L1* mRNA level was higher along with CTGF (encoded by CCN2 gene; i.e., a typical YAP1 downstream target [34,35]) in P4 hESCs than P1 hESCs (Fig. 4C). Despite similarities in YAP1 transcription, the YAP1 protein level was apparently stabilized with lower phosphorylated YAP1 (at S127) in P4 hESCs with higher TPX2 and TEAD4 expression (Fig. 4D). Consistently, nuclear YAP1 expression manifested along with TEAD4 protein expression in P4 hESCs (Fig. 4E). In contrast, depletion of YAP1 (Fig. 4F), TAZ (Fig. 4G), or TEAD4 (Fig. 4H) significantly decreased *BCL2L1* expression along with CTGF in P4 hESCs.

Aurora-A stabilizes the YAP1 protein

Previously, Aurora A, a mitotic kinase strongly associated with TPX2 for spindle assembly, was shown to phosphorylate and stabilize YAP1 in cancer [9,36]. Constant activation of Aurora-A, which corresponded with TPX2 induction regardless of cell cycle phase, was a distinct cellular phenotype of P3 and P4 hESCs [17]. P4 hESCs with high Aurora-A (determined by phospho-Aurora A) and TPX2 activities exhibited high protein levels of BCL-xL and YAP1 (Fig. 5A). As transient depletion of TPX2 also significantly lowered the protein level of BCL-xL (encoded by *BCL2L1*) and YAP1, high TPX2 induction in P4 hESCs would be closely associated to YAP dependent BCL2-xL expression (Fig. 5B). Next, to confirm the increased protein level of YAP1 results from protein stability, YAP1 protein was monitored after cycloheximide (CHX) treatment to inhibit protein translation in P1 and P4 hESCs (Fig. 5C). Similarly, the increased protein level of YAP1 was evident in Dox-dependent TPX2 induction (Fig. 5D), whereas the YAP1 mRNA level remained unaffected (Fig. 5E). Aurora-A active phosphorylation was clearly induced by TPX2 induction in iTPX2-hESCs, which was concurrent with the increase of YAP1 protein expression (Fig. 5F). Similar to P4 hESCs, YAP1 protein and not TEAD4 (Fig. S4B) was highly stabilized after Dox treatment in iTPX2-hESCs (Fig. 5G). These data suggest that high YAP1 protein levels in culture-adapted hESCs result from high Aurora-A activity by TPX2 induction.

Inhibition of Aurora-A abrogated the resistance to mitotic stress by YAP1 destabilization

Given that the activity of Aurora-A in hESCs with high TPX2 expression appeared to stabilize YAP1, we next tested whether chemical inhibition of Aurora-A may destabilize YAP1 and sensitize hESCs with high TPX2 expression to mitotic stress. To this end, we first determined the concentration of Aurora-A inhibitor (MLN8237: MLN) for inhibition of Aurora-A in hESCs with high TPX2 expression (P4 and iTPX2-hESCs with Dox). Intriguingly, Aurora-A activity determed by its active phosphorylation was significantly reduced by 50nM of MLN treatment in P1 hESCs (Fig. S5A), where it remained active up to 100nM in P4 hESCs (Fig. S5B). Clear attenuation of active phosphorylation in P4 hESCs was distinct from 0.5mM of MLN treatment (Fig. 6A). Therefore, all downstream experiments for survival test in P4 were performed using 0.5mM of MLN. In pararllel with Aurora-A inhibition by MLN (Fig. 6A), *BCL2L1* transcription was reduced along with *CTGF* and *SERPINE1* [34,37] (Fig. 6B). Mitotic resistance in P4 hESCs, as determined in the sub G1 and 3N populations, was also significantly attenuated by additional MLN treatment with Noc (Fig. 6C). The same result was reproduced by flow cytometry to determine the live cell population (Fig. 6D). Consistently, marked stabilization of YAP1 by Dox in iTPX2-hESCs was reversed by MLN treatment (Fig. 6E). The reduced YAP1 protein by MLN resulted from the destabilization of YAP1 protein by MLN (Fig. 6F), which further led to BCL-xL protein downregulation (Fig. 6G). Accordingly, MLN treatment significantly sensitized GFP positive population (expressing TPX2) to mitotic stress in iTPX2-hESCs (Fig. 6H).

Discussion

Despite the widespread concerns regarding the frequent genetic aberration and consequently acquired survival trait of hESCs[3], the molecular mechanisms underlying such drastic phenotypic changes have not been fully determined, except for the known role of *BCL2L1* induction followed by 20q11.21 CNV [8,10,11]. Here, we demonstrated that *BCL2L1* transcription was induced by stabilized YAP1 due to high Aurora-A activity via TPX2 induction at locus 20q11.21. Further, *BCL2L1* induction (Fig. 2) followed by YAP1 protein stabilization (Fig. 5) was readily achieved by inducible TPX2 induction without 20q11.21 CNV (Fig. 2l), resulting in survival under mitotic stress (Fig. 3). Therefore, 20q11.21 CNV itself would not be sufficient to lead to the survival trait. This result is consistent with a recent study that human iPSCs with 20q11.21 CNV only show the lesser commitment of the ectodermal lineage in teratoma without expression change in 20q11.21 loci [28]. Similarly, no drastic phenotypic changes (e.g., *BCL2L1* expression and survival trait) were observed in P2 hESCs with CNV at 20q11.21 (passage number of approximately 100), unlike P3 hESCs (passage number of approximately 200), which exhibited a clear *BCL2L1* expression and survival trait[8] along with high TPX2 expression and abnormal mitosis[17]. Therefore, we propose that other cues to activate *BCL2L1* promoter activity such as YAP1 activation would be required to confer the cells with the survival advantage trait (e.g., YAP1 stabilization by Aurora-A activity due to TPX2 induction). A recent study demonstrated that the Hedgehog signal is responsible for TPX2 induction through the FOXM1 transcription factor in cancer cells[30]. Considering the complexity of the YAP1 activation mechanism, we could not rule out the role of other events (e.g., F-actin stabilization [24]) in YAP1 activation for culture adaptation of hESCs other than the TPX2-Aurora-A axis. TPX2, of which basal expression was higher even in normal hESCs than differentiated cells [17], was critical for self-renewal of hESCs as stable depletion of TPX2 failed to be achieved multiple times (data not shown). Thus, only transient depletion of TPX2 with siRNA was performed. These results further support that TPX2 knockout leads to failure of early embryogenesis even prior to blastocyst formation [38]. As TPX2 induction stabilizes the mitotic spindle and leads to abnormal mitosis [17], TPX2 induction occurring in multiple culture-adapted cell lines [17] would serve as a potential driver not only for ‘acquired survival’ but also further ‘genetic alteration’ by saving hESCs from cell death after abnormal mitosis.

Unlike other somatic cells, hESCs are highly sensitive to genotoxic stress, which is believed to be a major safeguard system to ensure genome integrity [39]. This extremely high susceptibility to DNA damage is mostly triggered by high mitochondrial priming to apoptosis [16] through p53 mitochondrial translocation [13]. Thus, p53 dominant-negative mutation[12], *NOXA* mutation [9], and induction of *BCL2L1* [11] abrogate the unique genome safeguard mechanism of high mitochondrial priming, which occurs in culture-adapted hESCs. Therefore, the incidence of random mutations including CNV at 20q11.21 (where *TPX2* and *BCL2L1* are located) during prolonged culture to favor survival through TPX2 induction to activate YAP1 dependent *BCL2L1* induction in hESCs with 20q11.21 CNV would be sufficient for dominant selection during multiple bottleneck events [40]. Thus, continuous loss of high mitochondrial priming and building resistance to mitotic stress may collectively enhance chromosome instability and even induce aneuploidy during long-term hESC culture.

Conclusion

CNV at locus 20q11.21 was not sufficient to lead to culture adaptation. Further, TPX2 induction and subsequent activation of Aurora-A stabilizes YAP1 to promote *BCL2L1* transcription from an amplified 20q11.21 locus, thus promoting the survival trait in hESCs.

Declarations

***Avaiablity of data and material*:** Source data are available from the corresponding authors upon request. The RNAseq results have been deposited to Gene Expression Omnibus (GEO) under accession number GSE 167495. The flow cytometery data was deposited to https://flowrepository.org/id/FR-FCM-Z435.

Acknowledgements: We thank Dr. Minh Dang Nguyen at the University of Calgary for kindly providing TPX2 constructs.

Funding: This work was supported by a grant from the National Research Foundation of Korea (NRF) (grant number 2020M3A9E4037905, 2020R1A2C2005914).

Author contributions

HJ.C conceived the overall study design and led the experiments and wrote the manuscript. YJ.K conducted the experiments, data analysis and wrote the first draft. HC.J provided the key preliminary data, YH.G generated cell lines and performed the initial characterization. HS.C, HD.S, and H.L provided array data and performed data analysis. All authors contributed to manuscript writing and revising and endorsed the final version of this manuscript.

Correspoindng authors

Correspondence to Hyuk-Jin Cha (hjcha93@snu.ac.kr)

Ethics declarations

Conflict interests: The authors declare that they have no known competing financial interests or personal relationships that could have appeared to influence the work reported in this paper.

Supplementary data

Supplementary data are available at Cellular and Molecular Life Science online.

References

1. Lund RJ, Narva E, Lahesmaa R (2012) Genetic and epigenetic stability of human pluripotent stem cells. Nat Rev Genet 13:732–744

2. Heslop JA et al (2015) Concise review: workshop review: understanding and assessing the risks of stem cell-based therapies. Stem Cells Transl Med 4:389–400
3. Andrews PW et al (2017) Assessing the Safety of Human Pluripotent Stem Cells and Their Derivatives for Clinical Applications. Stem Cell Reports 9:1–4
4. Halliwell J, Barbaric I, Andrews PW (2020) Acquired genetic changes in human pluripotent stem cells: origins and consequences. Nat Rev Mol Cell Biol 21:715–728
5. Baker DE et al (2007) Adaptation to culture of human embryonic stem cells and oncogenesis in vivo. Nat Biotechnol 25:207–215
6. Spits C et al (2008) Recurrent chromosomal abnormalities in human embryonic stem cells. Nat Biotechnol 26:1361–1363
7. Lefort N, Feyeux M, Bas C, Feraud O, Bennaceur-Griscelli A, Tachdjian G, Peschanski M, Perrier AL (2008) Human embryonic stem cells reveal recurrent genomic instability at 20q11.21. Nat Biotechnol 26:1364–1366
8. Cho SJ et al (2018) Selective Elimination of Culture-Adapted Human Embryonic Stem Cells with BH3 Mimetics. Stem Cell Reports
9. Zhang J et al (2019) Anti-apoptotic Mutations Desensitize Human Pluripotent Stem Cells to Mitotic Stress and Enable Aneuploid Cell Survival. Stem Cell Reports 12:557–571
10. Nguyen HT, Geens M, Mertzanidou A, Jacobs K, Heirman C, Breckpot K, Spits C (2014) Gain of 20q11.21 in human embryonic stem cells improves cell survival by increased expression of Bcl-xL. Mol Hum Reprod 20:168–177
11. Avery S et al (2013) BCL-XL mediates the strong selective advantage of a 20q11.21 amplification commonly found in human embryonic stem cell cultures. Stem Cell Reports 1:379–386
12. Merkle FT et al (2017) Human pluripotent stem cells recurrently acquire and expand dominant negative P53 mutations. Nature 545:229–233
13. Lee MO et al (2013) Inhibition of pluripotent stem cell-derived teratoma formation by small molecules. Proc Natl Acad Sci U S A 110:E3281–E3290
14. TeSlaa T, Setoguchi K, Teitell MA (2016) Mitochondria in human pluripotent stem cell apoptosis. Semin Cell Dev Biol 52:76–83
15. Dumitru R, Gama V, Fagan BM, Bower JJ, Swahari V, Pevny LH, Deshmukh M (2012) Human Embryonic Stem Cells Have Constitutively Active Bax at the Golgi and Are Primed to Undergo Rapid Apoptosis. Mol Cell
16. Liu JC et al (2013) High mitochondrial priming sensitizes hESCs to DNA-damage-induced apoptosis. Cell Stem Cell 13:483–491
17. Jeong H-C et al (2021) TPX2 Amplification-Driven Aberrant Mitosis in Long-Term Cultured Human Embryonic Stem Cells. bioRxiv, 2021.02.22.432205
18. Lamm N, Ben-David U, Golan-Lev T, Storchova Z, Benvenisty N, Kerem B (2016) Genomic Instability in Human Pluripotent Stem Cells Arises from Replicative Stress and Chromosome Condensation

Defects. Cell Stem Cell 18:253–261

19. Thompson O et al (2020) Low rates of mutation in clinical grade human pluripotent stem cells under different culture conditions. Nat Commun 11:1528
20. Liu JC, Lerou PH, Lahav G (2014) Stem cells: balancing resistance and sensitivity to DNA damage. Trends Cell Biol 24:268–274
21. Morin-Kensicki EM et al (2006) Defects in Yolk Sac Vasculogenesis, Chorioallantoic Fusion, and Embryonic Axis Elongation in Mice with Targeted Disruption of Yap65. Mol Cell Biol 26:77–87
22. Lian I et al (2010) The role of YAP transcription coactivator in regulating stem cell self-renewal and differentiation. Genes Development 24:1106–1118
23. Leblanc L et al (2018) Yap1 safeguards mouse embryonic stem cells from excessive apoptosis during differentiation. eLife 7:1–26
24. Ohgushi M, Minaguchi M, Sasai Y (2015) Rho-Signaling-Directed YAP/TAZ Activity Underlies the Long-Term Survival and Expansion of Human Embryonic Stem Cells. Cell Stem Cell
25. Rosenbluh J et al (2012) β-Catenin-driven cancers require a YAP1 transcriptional complex for survival and tumorigenesis. Cell 151:1457–1473
26. Kim KT et al (2020) Safe scarless cassette-free selection of genome-edited human pluripotent stem cells using temporary drug resistance. Biomaterials 262:120295
27. Go YH et al (2019) Structure-Activity Relationship Analysis of YM155 for Inducing Selective Cell Death of Human Pluripotent Stem Cells. Front Chem 7:298
28. Jo HY et al (2020) Functional in vivo and in vitro effects of 20q11.21 genetic aberrations on hPSC differentiation. Sci Rep 10:18582
29. Blum B, Bar-Nur O, Golan-Lev T, Benvenisty N (2009) The anti-apoptotic gene survivin contributes to teratoma formation by human embryonic stem cells. Nat Biotechnol 27:281–287
30. Wang Y et al (2020) The critical role of dysregulated Hh-FOXM1-TPX2 signaling in human hepatocellular carcinoma cell proliferation. Cell Commun Signal 18:116
31. Warner SL et al (2009) Validation of TPX2 as a potential therapeutic target in pancreatic cancer cells. Clin Cancer Res 15:6519–6528
32. Reid TA et al (2016) Suppression of microtubule assembly kinetics by the mitotic protein TPX2. J Cell Sci 129:1319–1328
33. Meyer-Ficca ML, Meyer RG, Kaiser H, Brack AR, Kandolf R, Kupper JH (2004) Comparative analysis of inducible expression systems in transient transfection studies. Anal Biochem 334:9–19
34. Zhao B et al (2008) TEAD mediates YAP-dependent gene induction and growth control. Genes Dev 22:1962–1971
35. Hansen CG, Moroishi T, Guan KL (2015) YAP and TAZ: A nexus for Hippo signaling and beyond. Trends Cell Biol 25:499–513
36. Chang SS et al (2017) Aurora A kinase activates YAP signaling in triple-negative breast cancer. Oncogene 36:1265–1275

37. Choi JY, Lee H, Kwon EJ, Kong HJ, Kwon OS, Cha HJ (2021) TGFbeta promotes YAP-dependent AXL induction in mesenchymal-type lung cancer cells. Mol Oncol 15:679–696
38. Aguirre-Portoles C, Bird AW, Hyman A, Canamero M, Perez de Castro I, Malumbres M (2012) Tpx2 controls spindle integrity, genome stability, and tumor development. Cancer Res 72:1518–1528
39. Weissbein U, Benvenisty N, Ben-David U (2014) Genome maintenance in pluripotent stem cells. J Cell Biol 204:153–163
40. Barbaric I, Biga V, Gokhale PJ, Jones M, Stavish D, Glen A, Coca D, Andrews PW (2014) Time-lapse analysis of human embryonic stem cells reveals multiple bottlenecks restricting colony formation and their relief upon culture adaptation. Stem Cell Reports 3:142–155

Tables

Table 1. RT-qPCR primer sequence

Gene symbol	Primer sequence (5' to 3')
18srRNA	F : GTA ACC CGT TGA ACC CCA TT R : CCA TCC AAT CGG TAG TAG CG
TPX2	F : GCT CAA CCT GTG CCA CAT TA R : CGA GAA AGG GCA TAT TTC CA
eGFP	F : CCG GAC CTC CAA AGA AAA A R : AAA AGT GAC CCC CGA CCT T
BCL2L1	F : GAT CCC CAT GGC AGC AGT AAA GCA AG R : CCC CAT CCC GGA AGA GTT CAT TCA CT
BIRC5	F: GGA CCA CCG CAT CTC TAC R: GCA CTT TCT TCG CAG TTT
YAP	F: GTG AGC CTG TTT GGA TGA TG R: CAC TGG ACA AAG GAA GCT GA
TAZ	F : CCA GGT GCT GGA AAA AGA AG R : CAG GAT GAT GGG GTT GAG AT
CTGF	F : CCA ATG ACA ACG CCT CCT G R : TGG TGC AGC CAG AAA GCT C
SERPINE1	F: TTG AAT CCC ATA GCT GCT TGA AT R: ACC GCA ACG TGG TTT TCT CA
TEAD4	F: GAA CGG GGA CCC TCC AAT G R: GCG AGC ATA CTC TGT CTC AAC

Table 2. siRNA sequence

Gene Symbol	siRNA sequence (5' to 3')
TPX2	S : CAG GAU UUU GCU GUG AAG U AS : ACU UCA CAG CAA AAU CCU G
TEAD4	S : CCG CCA AAU CUA UGA CAA ATT AS : UUU GUC AUA GAU UUG GCG GTT
YAP	S : CAG AAG AUC AAA GCU ACU U AS : AAG UAG CUU UGA UCU UCU G
TAZ	S : ACG UUG ACU UAG GAA CUU U AS : AAA GTT CCT AAG TCA ACG T

Figures

Figure. 1

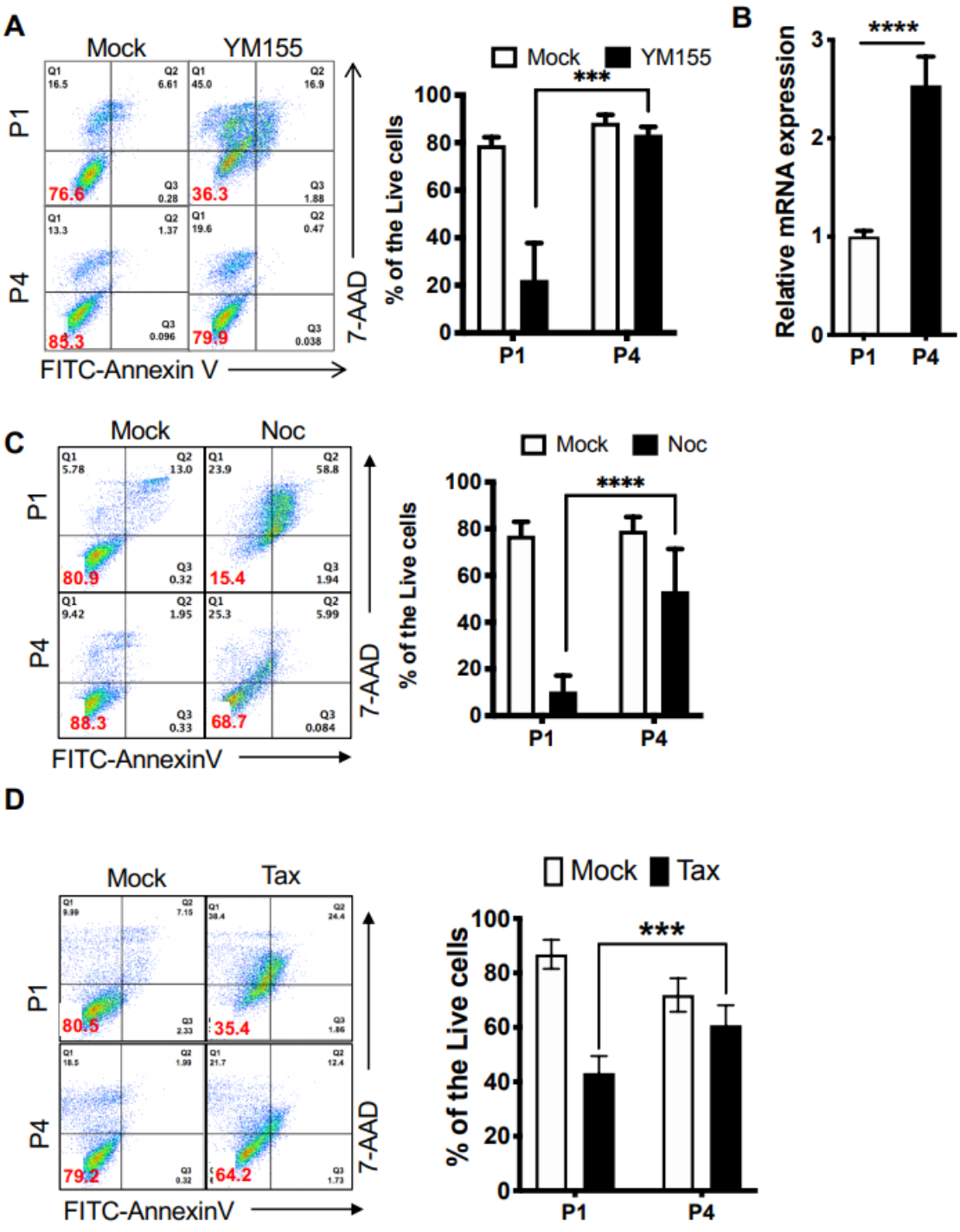

Figure 1

Survival advantage of culture adapted hESCs under mitotic stress (A) After treatment of YM155 (50nM), cell death of P1 and P4 hESCs was determined by AnnexinV/7-AAD staining. (two-way ANOVA. n=6, p = 0.0004.) (B) Relative mRNA level of BCL2L1 in P1 and P4 hESCs (C-D) Cell death of P1 and P4 hESCs after treatment of 50ng/ml of nocodazole (Noc: C) or 50ng/ml of paclitaxel (Tax: D) was measured by flow cytometery, stained by AnnexinV/7-AAD staining. (Two-way ANOVA, n=5, p<0.0001)

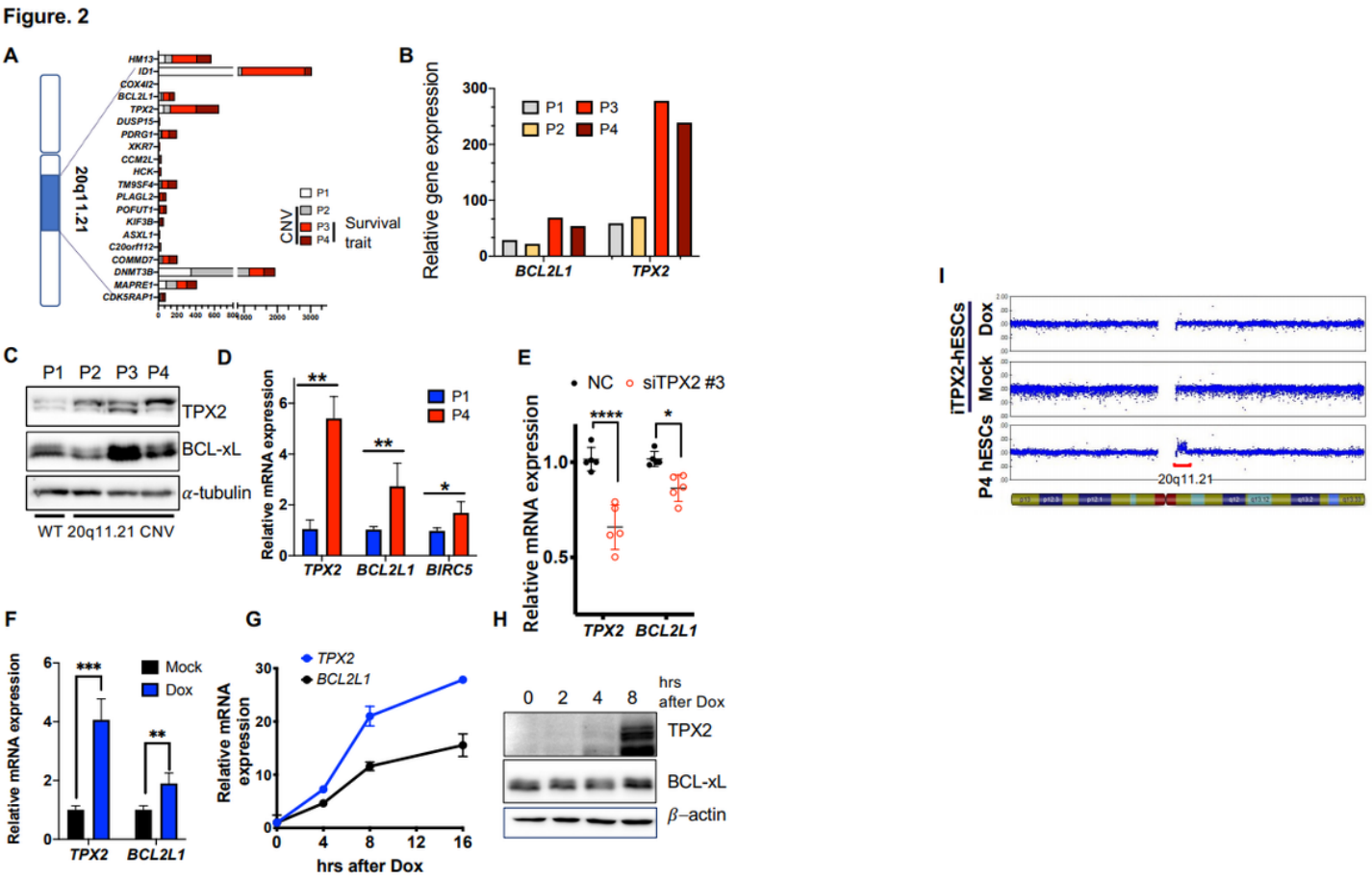

Figure 2

BCL2L1 induced survival associated with TPX2 (A) Graphical presentation of chromosome 20 and 20q11.21 locus with accompanied genes (left), Relative expression level of genes at 20q.11.21 locus in P1, P2, P3, and P4 hESCs (right) (B) Relative transcript of BCL2L1 and TPX2 in P1, P2, P3, and P4 hESCs. (C) Immunoblotting for TPX2 and BCL-xL of the indicated hESCs, α-tubulin for equal protein loading. (D) The relative mRNA expression level of the indicated gene in P1 and P4 hESCs. (n=7, unpaired t-test, p-value = 0.0039 for TPX2, 0.0028 for BCL2L1, and 0.0152 for BIRC5). (E) Relative mRNA expression level of TPX2 and BCL2L1 in P4 hESCs 48 hours after siRNA for control (NC) and TPX2 (siTPX2#3) (n=5, 2-Way ANOVA, p-value <0.0001 for TPX2, 0.0125 for BCL2L1) (F) Relative mRNA expression level of TPX2 and BCL2L1 at 24 hours after treatment of 0.1 μg/ml of Dox treatment in H9-iTPX2-hESC (n=4, 2-Way ANOVA, p-value < 0.0001 for TPX2, and 0.0393 for BCL2L1) (G) Relative mRNA expression level of TPX2 or BCL2L1 at indicated time after 0.1 μg/ml of Dox treatment in iTPX2-hESCs. (H) Immunoblotting of TPX2 and BCL-xL at indicated time after 0.1 μg/ml of Dox treatment in iTPX2-hESCs (I) Copy number output using the Illumina Asian Screening Array (~700K) as computed by GenomeStudio software provided by Illumina. The two plots shown are for B allele frequency and log R ratio. The copy number gain on chromosome 20 detected in H9-P4 hESCs based on log R ratio is shown by a red bar.

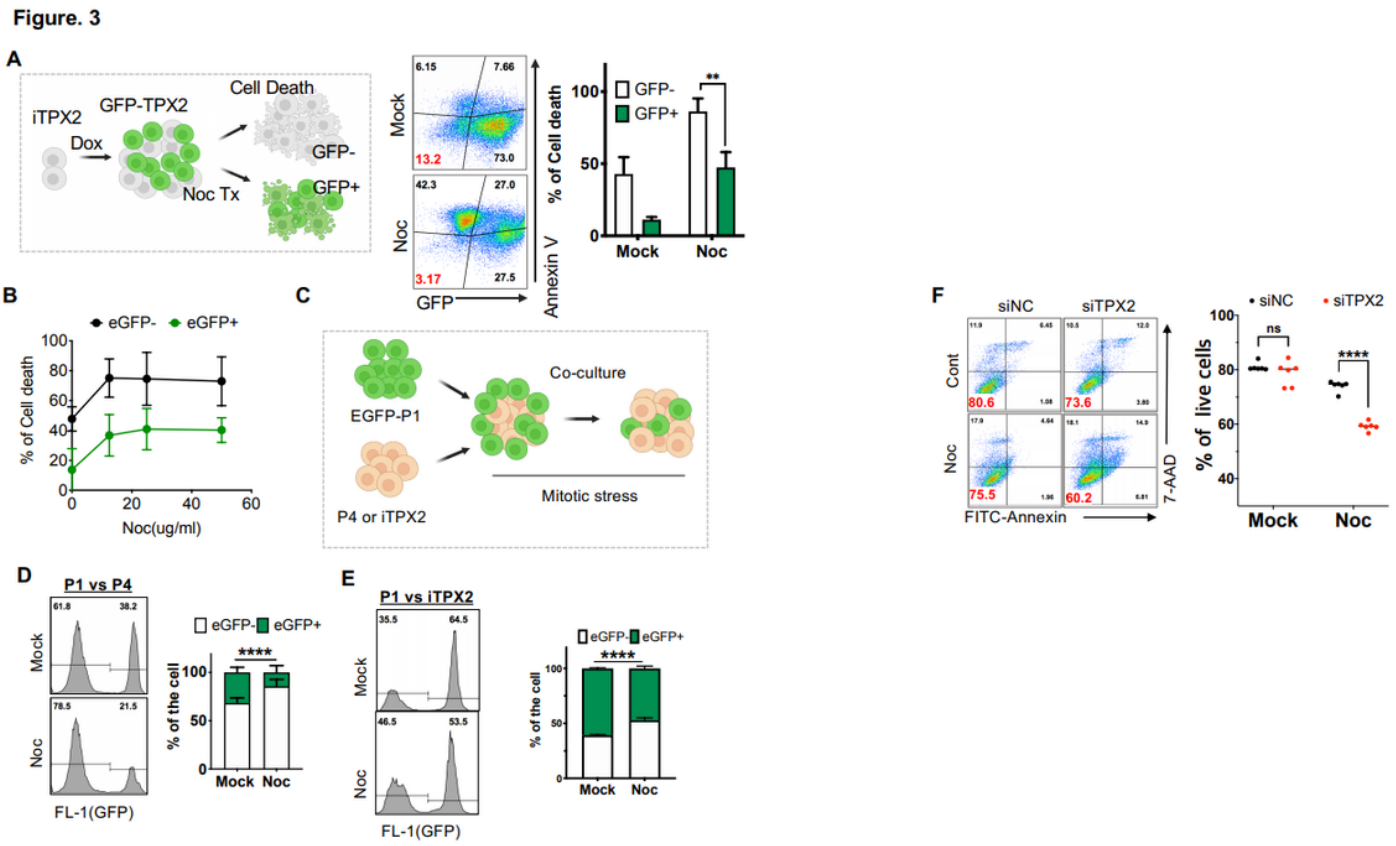

Figure 3

TPX2 induction rescues mitotic cell death of normal hESCs (A) Graphical presentation of the assay (left panel), Flow cytometry of AnnexinV/7-AAD co-staining after 0.1 μg/ml Dox pretreatment for 16hr in iTPX2 hESCs in the presence or absence of nocodazole (50ng/ml) (Noc Tx), Graphical presentation of cell death (%) of GFP negative and positive cell (right panel) (B) Nocodazole dose-dependent survival determined by AnnexinV/7-AAD co-staining of GFP negative or positive population (C) Graphical presentation of competition assay (D and E) Flow cytometry of P1 and P4 hESCs (D, n=6) or P1 and iTPX2 hESCs (E, n=5) after treatment of 50ng/ml of Nocodazole for 24hr. Populations were identified by GFP after 2 days of Nocodazole treatment. (F) Flow cytometry of AnnexinV/7-AAD co-staining of P4 hESCs after control (siNC) or TPX2 siRNA (siTPX2) introduction to P4 hESCs was tested. n=6, 2-way ANOVA, p-value<0.0001 for Noc treated siNC VS Noc treated siTPX2, p-value = 0.0011 for Noc untreated siNC VS Noc untreated siTPX2.

Figure. 4

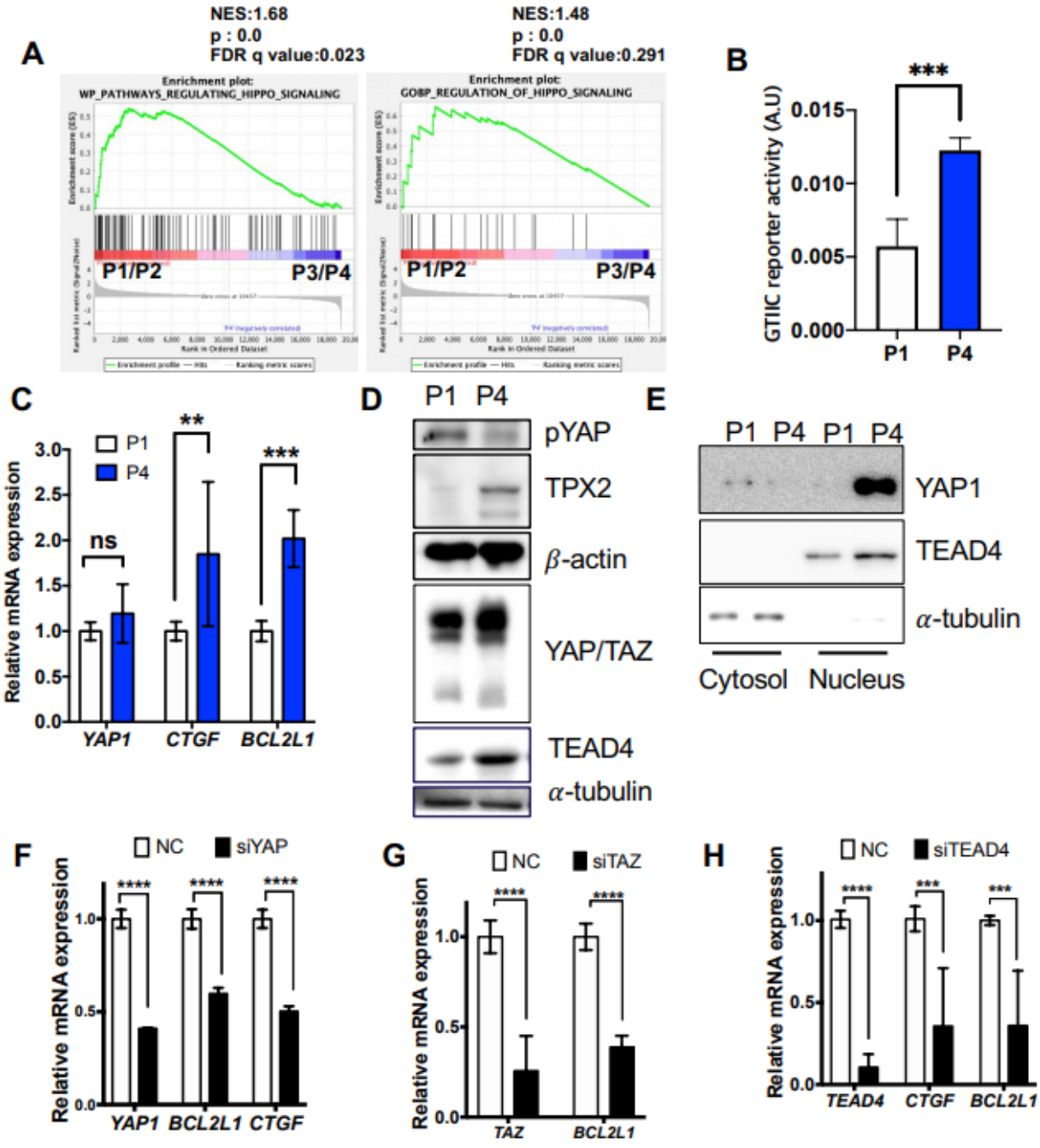

Figure 4

YAP/TEAD4 leads to BCL2L1 expression (A) GSEA analysis of WP_PATHWAYS_REGULATING_HIPPO_SIGANLING (left) and GOBP_REGULATION_OF_HIPPO_SIGNALING (right) of P1/P2 hESCs and P3/P4 hESCs from RNAseq data of P1, P2, P3 and P4 hESCs (GSE167495) (B) 8X GTIIC reporter assay of P1 and P4 hESCs (n=4, Unpaired t-test, p-value = 0.0007) (C) Relative mRNA level of YAP1, CTGF and BCL2L1 of P1 or P4 hESCs (n=6, 2-Way ANOVA, ns:not significant, p-value

for CTGF = 0.0068, BCL2L1 = 0.0009) (D) Immunoblotting of TPX2, YAP1, TEAD4 and phosphorylation of YAP1 (serine 127: pYAP), α-tubulin or β-actin for equal protein loading. (E) Immunoblotting of YAP1 and TEAD4 of cytosol or nucleus from P1 or P4 hESCs, α-tubulin for equal protein loading (F-H) Relative mRNA expression in P4 of indicated genes after control (NC) or siRNA of YAP1 (F), TAZ (G) or TEAD4 (H) (F) n=6, p-value for YAP1, BCL2L1, and CTGF <0.0001. (G) n=4 for NC, 6 for siTAZ. p-value for YAP1 and BCL2L1 <0.0001. (H) n=5, p-value for TEAD4 <0.0001, 0.0005 for CTGF, and 0.0006 for BCL2L1.

Figure. 5

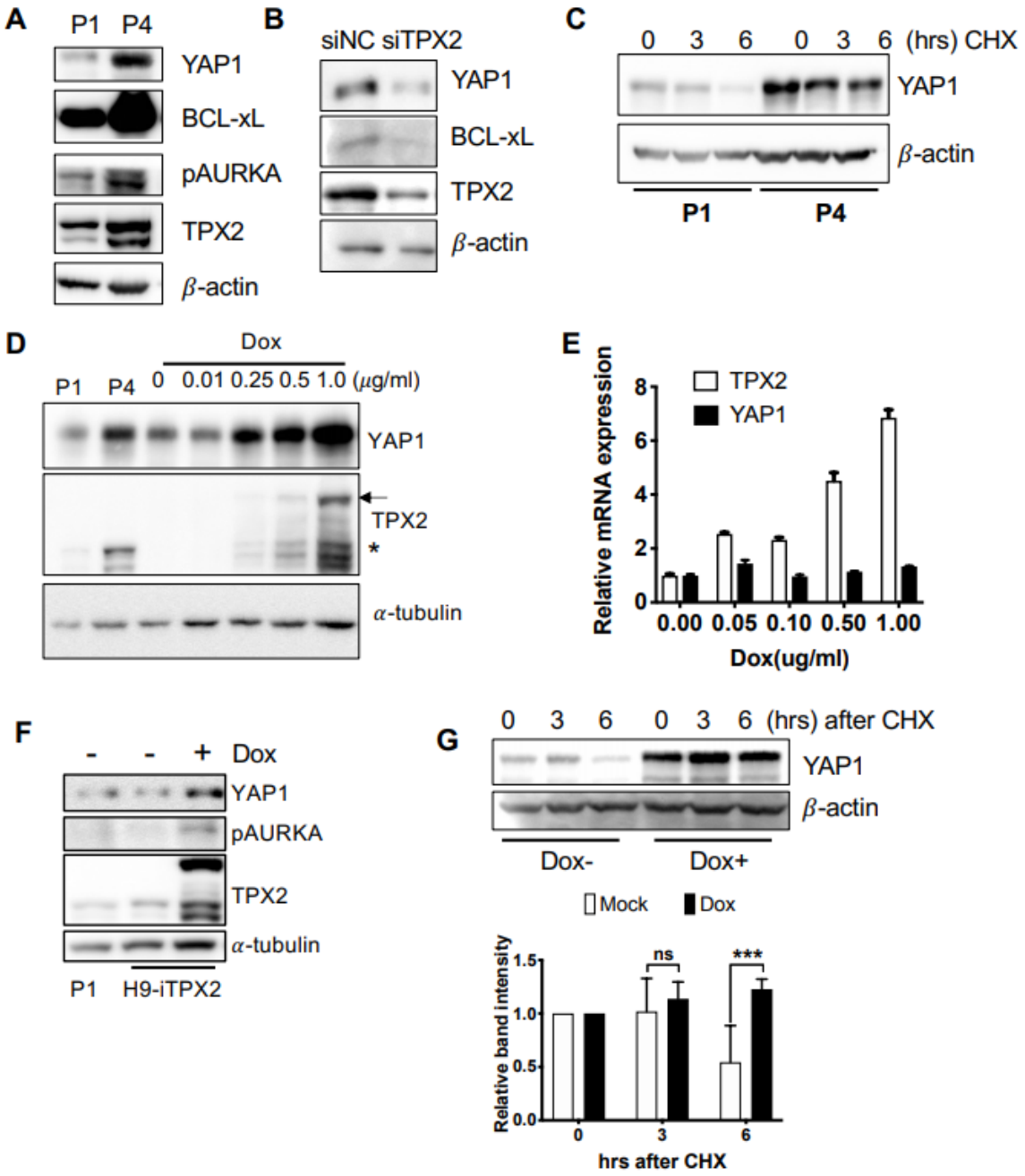

Figure 5

Aurora-A stabilizes YAP1 protein (A) Immunoblotting of YAP1, BCL-xL, TPX2, and phospho-Aurora A (pAURKA) in P1 and P4 hESCs, β-actin as a loading for equal protein (B) Immunoblotting of YAP1, BCL-xL, and TPX2 in P4 hESCs 2 days after introduction control (siNC) and TPX2 (siTPX2) siRNA, β-actin as a loading for equal protein (C) Immunoblotting of YAP1 of P1 or P4 hESCs after 200 μg/ml of cycloheximide(CHX) treatment, β-actin as a loading for equal protein (D) Immunoblotting for YAP1 or TPX2 after indicated dose of Dox treatment for 24hr(arrow for induced GFP-TPX2, * for endogenous TPX2), α-tubulin for equal protein loading. (E) The relative level of mRNA of TPX2 or YAP1 at the indicated dose of Dox for 24hr in H9-iTPX2. (F) Immunoblotting of YAP1, TPX2, and phospho-Aurora A (pAURKA) after 24hr treatment of Dox 0.1 μg/ml (G) Immunoblotting of YAP1 in iTPX2-hESCs with or without Dox 0.1μg/ml at indicated time after 200μg/ml of CHX treatment, , β-actin as a loading for equal protein (top), Graphical presentation of normalized band intensity from 4 independent experiments (ns:not significant, p-value = 0.0005 for 6hrs after CHX treatment)

Figure. 6

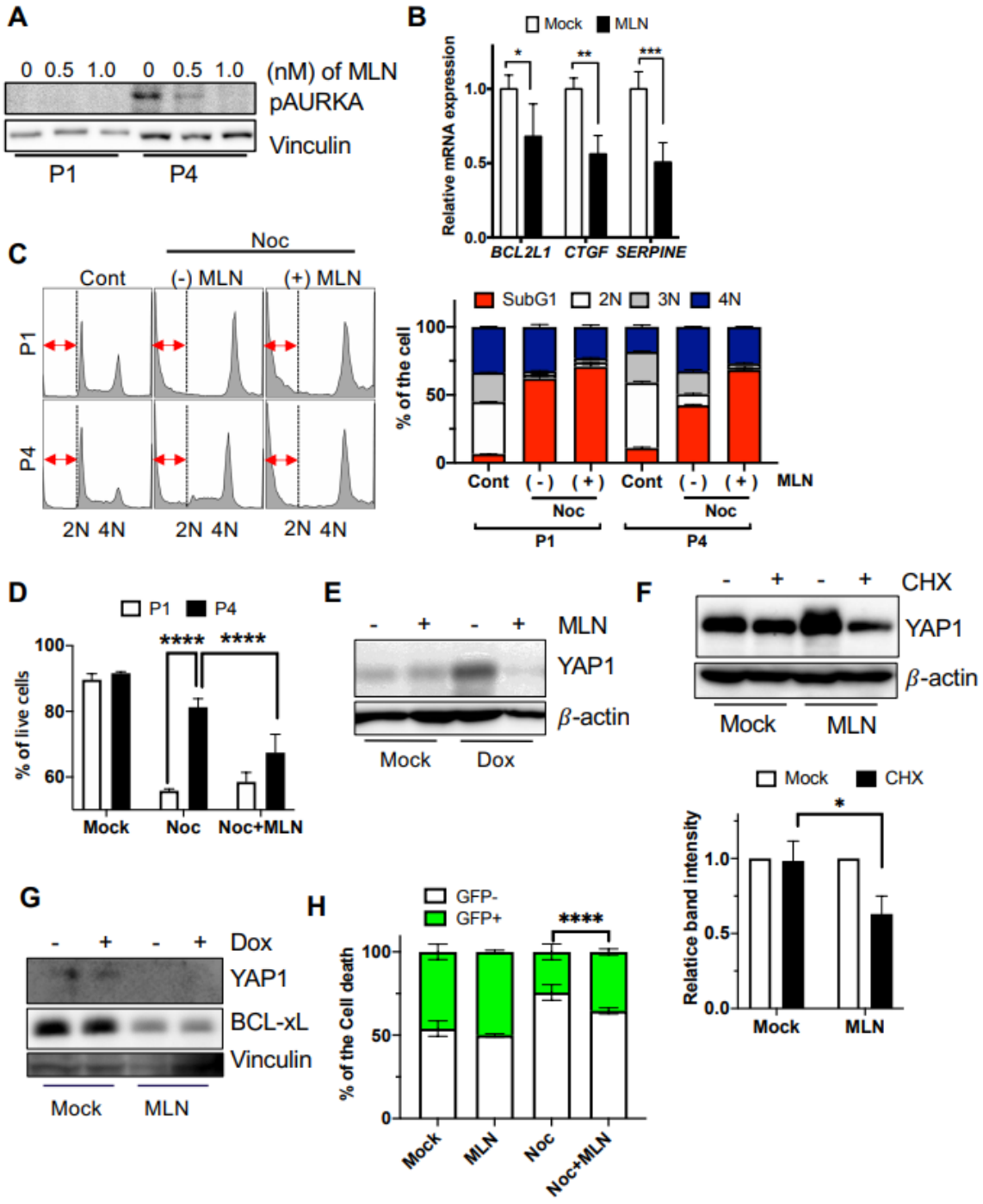

Figure 6

Inhibition of Aurora-A abrogated the resistance to mitotic stress by YAP1 destabilization (A) Immunoblotting for phospho-Aurora A (pAURKA) after treatment of indicated dose of MLN8237 (MLN) in P1 or P4 hESCs, Vinculin as the loading control. (B) Relative mRNA levels in P4 hESCs after 24hr of MLN 0.5μM treatment (n=4, 2-Way ANOVA, p-value for BCL2L1 = 0.0342, CTGF = 0.0025, SERPINE = 0.0007) (C) Flow cytometry of DNA contents, sub G1 population (red arrow) was presented after treatment of

nocodazole (Noc: 50 ng/ml) for 24hr with or without 0.5μM of MLN (left), Graphical presentation of each phase of cell cycle (right). (D) Cell death was quantified by FACS after 4hr pre-treatment of MLN, Nocodazole 50ng/ml were treated with or without 0.5μM MLN for 24hrs. n=6, 2-way ANOVA. p-value = 0.0011 for P1 Noc VS P4 Noc, p-value = 0.0177 for P4 Noc VS Noc+MLN. (E-F)Immunoblotting for YAP1 in iTPX2-hESCs. (E) After 24hr treatment of Dox 0.1 μg/ml, MLN 0.5μgM was treated for 24hrs. β-actin for equal loading control. (F) Protein stability of YAP1at 6 hours after treatment of CHX (TPX2 induction by 0.1μg/ml for 24 hours prior to the experiment and then 0.5μgM of MLN was pretreated at 1 hour prior to CHX treatment). Normalized YAP1 protein band intensity was shown from three independent experiments. (G) Immunoblotting for YAP1 or BCL-xL in iTPX2-hESCs at 24 hours after 0.5μM of MLN treatment. (H) The relative level of the live cell population of GFP positive or negative population in iTPX2-hESCs. n=4, 2-way ANOVA. P-value <0.0001 for GFP- and + Noc VS Noc+MLN.

Supplementary Files

This is a list of supplementary files associated with this preprint. Click to download.

- Supplementalmaterials.pdf